

DOPED H₂-FILLED RF CAVITIES FOR MUON BEAM COOLING*

K. Yonehara[†], M. Chung, A. Jansson, M. Hu, A. Moretti, M. Popovic, Fermilab, Batavia IL, USA
 M. Alsharo'a, R.P. Johnson, M. Neubauer, R. Sah, Muons Inc, Batavia, IL, USA
 D. V. Rose, C. Thoma, Voss Scientific, Albuquerque, NM USA

Abstract

RF cavities pressurized with hydrogen gas may provide effective muon beam ionization cooling needed for muon colliders. Recent 805 MHz test cell studies reported below include the first use of SF₆ dopant to reduce the effects of the electrons that will be produced by the ionization cooling process in hydrogen or helium. Measurements of maximum gradient in the Paschen region are compared to a simulation model for a 0.01% SF₆ doping of hydrogen. The observed good agreement of the model with the measurements is a prerequisite to the investigation of other dopants.

INTRODUCTION

Ionization cooling requires low-atomic-number energy absorbers immersed in a strong magnetic field and high-gradient, large-aperture RF cavities to be able to cool a muon beam as quickly as the short muon lifetime requires. RF cavities pressurized with dense hydrogen gas are being developed to use the same real estate to provide the energy absorber and the RF acceleration needed for ionization cooling, where the absorption of dark currents by the dense gas will allow the cavities to operate in strong magnetic fields. The same test cell that is used in the experiments reported here has been used to show that a pressurized cavity is not affected by an external magnetic field [1]. The next step is to subject the cavity to an intense 400 MeV proton beam in the Muon Test Area (MTA) at Fermilab.

The behavior of a pressurized RF cavity has been the subject of modeling studies [2] which have pointed out that the recombination time of the electrons that are ionized by the muon beam in a cooling channel may not be fast enough. That is, the electrons may survive for many RF cycles, transferring their energy to the hydrogen gas and effectively reducing the cavity quality factor such that an impossible amount of RF power is required. If this is the case, one solution is to add to the gas an electronegative dopant to capture the free electrons to increase their effective mass. The resulting heavy ions would not move enough during an RF cycle to transfer significant energy to the gas.

Numerical simulations have previously been compared to test cell breakdown behavior in the Paschen region [3]. In this report, new measurements of SF₆-doped hydrogen gas breakdown are compared with new simulations. Studies of RF breakdown at higher pressures due to electrode material are discussed in another paper [4].

EQUIPMENT

A schematic of the 805 MHz Test Cell (TC) geometry is shown in Figure 1. The TC is a cylindrical copper-plated stainless steel pressure vessel. RF power is fed into the chamber via a coaxial line. Replaceable hemispherical electrodes of various materials (Sn, Al, Cu, Mo, Be, W) are separated by a 2 cm gap. The characteristics of the cavity and the MTA experimental conditions have been described previously [1].

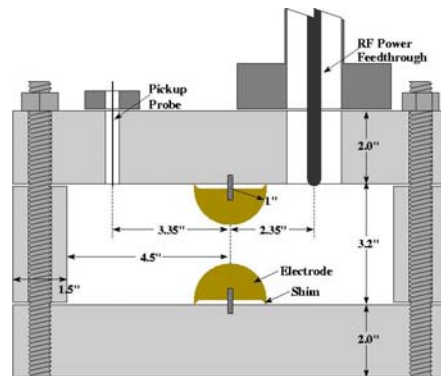


Figure. 1: Cross section of the test cell showing the replaceable one-inch radius Sn, Al, Cu, Mo, W, or Be hemispherical electrodes.

EXPERIMENTAL RESULTS

Copper electrode

Figure 2 shows the maximum stable surface gradient with copper electrodes using nitrogen, hydrogen, and one part in 10⁴ SF₆ doped hydrogen gas as a function of gas pressure. The plotted field gradient is scaled from the calibrated pickup signal based on a Superfish model of the TC. Two breakdown regions are seen in the plots. In the lower pressure, or gas breakdown, region the maximum stable gradient increases linearly as a function of gas pressure as predicted by Paschen's law. The slope of gradient over pressure, E/p, is determined by the gas species. The observed slopes are shown in Table 1.

In higher pressure region, the breakdown voltage is not dependent on the gas pressure. The maximum voltage depends on the characteristics of electrode material. Hence, we refer to this region as the surface breakdown region. The observed plateau levels are shown in Table 1 and discussed elsewhere [4].

*Work supported in part by USDOE STTR Grant DE-FG02-08ER86350 and FRA DOE contract number DE-AC02-07CH11359

[†]yonehara@fnal.gov

Other electrode materials

Similar measurements were done with aluminum and tin electrodes. Table 1 shows the summary of all electrode measurements. Figures 3 and 4 show the observed breakdown gradients with aluminum and tin electrodes, respectively.

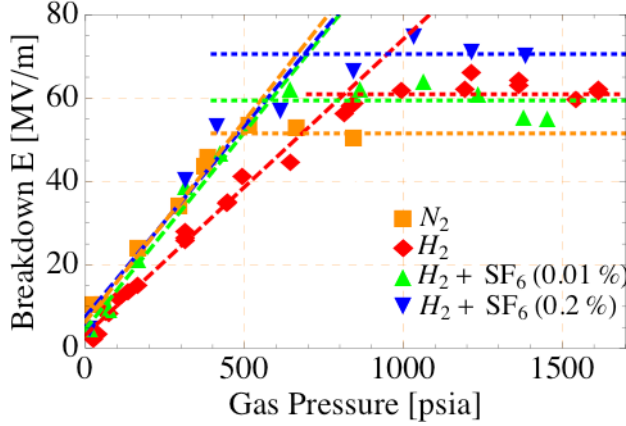


Figure 2: Observed breakdown as a function of gas pressure in copper electrodes with various gases.

Table 1: Observed E/p and maximum electric field

Copper	E/p [MV/m/psia]	Max E [MV/m]
N2	0.096	52
H2	0.071	61
H2+SF6 (0.01 %)	0.094	59
H2+SF6 (0.2 %)	0.091	71
Aluminum	E/p [MV/m/psia]	Max E [MV/m]
H2	0.059	54
H2+SF6 (0.01 %)	0.105	61
Tin	E/p [MV/m/psia]	Max E [MV/m]
H2	0.057	38
He	0.0093	
He+SF6 (0.1 %)	0.013	

Systematic error in breakdown measurement

The dominant breakdown process in the gas breakdown region is the electromagnetic interaction between electrons and gas molecules. The electrode material effect is small in this region. A systematic error can be estimated based on this assumption by comparing results for different electrodes. The E/p slopes for Al and Sn are close each other while the E/p for Cu is 20 % higher. On the other hand, the ratio of E/p slopes between Cu and Al in H₂ + SF₆ (0.01 %) is 10 %.

The large systematic error in the slope determination is caused by the difficulty to measure the pickup voltage at small pressure and the difficulty to know the transition point between gas and surface breakdown regions at higher pressures. However, in the comparison of the simulations with the data in the next section, we will compare values in the center of the gas breakdown region

at 325 psia, where the end effects of the slope determination are not involved.

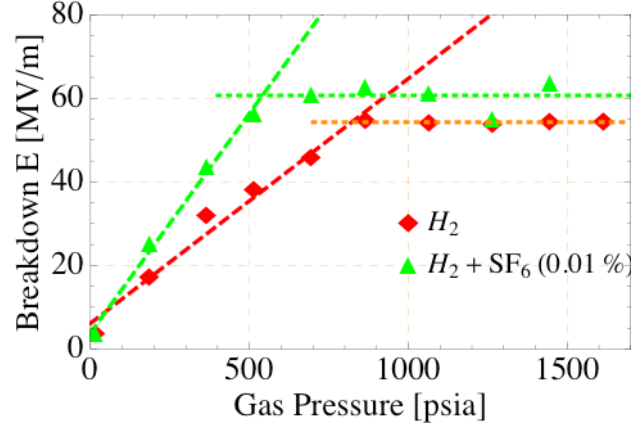


Figure 3: Observed breakdown as a function of gas pressure in aluminum electrodes.

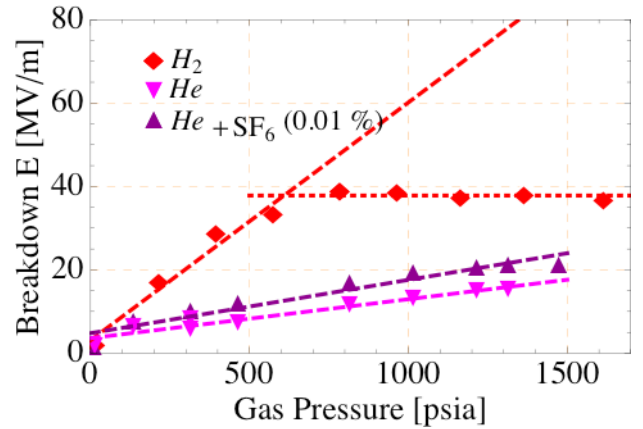


Figure 4: Observed breakdown as a function of gas pressure in tin electrodes.

SIMULATION RESULTS

Computer calculations to simulate the behavior of breakdown in helium-filled spark-gap switches [5] have been extended to use hydrogen and SF₆ [6] in the Muons, Inc. Test Cell [7]. Three values of electric field were used for the calculations in the conditions of Figure 2 for hydrogen gas (red diamonds) at a density of .002 g/cm³, near 325 psia.

Figure 5 shows the simulation results for the three electric field strengths, where the electron density is stable below the Paschen curve (10 MV/m), slightly unstable at the curve (25 MV/m), and very unstable for values above the curve (50 MV/m).

The temporal evolution of these curves is consistent with the results of the experiment; for $E_0 = 10$ MV/m, the electron population does not grow because the field is too low to induce ionization of the neutral H₂. At 25 MV/m, the electron density is slowly growing, consistent with this value of E_0 being at the edge of the Paschen law breakdown limit in Figure 2. At 50 MV/m, the electric field drives electrons in the tail of the distribution to high enough energies to efficiently ionize the gas. It is

interesting that the 805 MHz period is seen in the growth of the electron density.

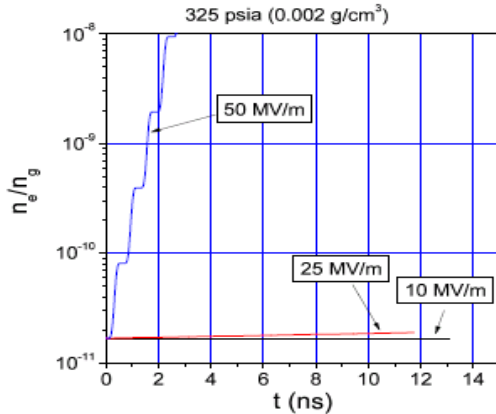


Figure 5: Electron density as a function of time at 805 MHz and gas density 0.002 g/cm^3 .

One proposed method to increase the effective breakdown threshold for the gas at a given pressure is to introduce a low concentration of electro-negative gas to the H_2 . A very low ratio mixture of SF_6 was used to examine this effect. Three additional processes of neutral SF_6 , SF_6^+ , and SF_6^- were added to the calculation. Figure 6 shows the calculated breakdown field in H_2 and $\text{H}_2 + \text{SF}_6$ (0.01 %) gas conditions. The simulation result agrees well with the experimental result.

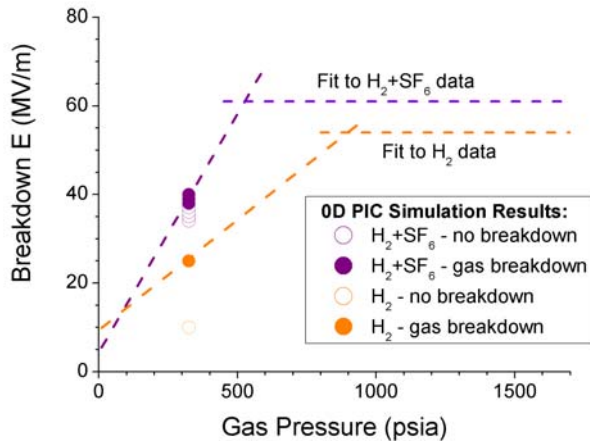


Figure 6: Calculated breakdown fields in H_2 or $\text{H}_2 + \text{SF}_6$ (0.01 %) at 325 psia. The broken lines are fits using the aluminum electrode data. Solid or open circles represent RF breakdown or no breakdown, respectively.

Since a general simulation of gas breakdown dynamics requires significant computational power, some interactions are not explicitly included in the model. For instance, the electron attachment process in neutral hydrogen ($\text{H}_2 + e \rightarrow \text{H}^- + \text{H}^0$) is not taken into account since it has a relatively small cross-section. The simulations are initialized with a small seed population of electrons (with number density $\sim 10^{-10}$ of the neutral gas density).

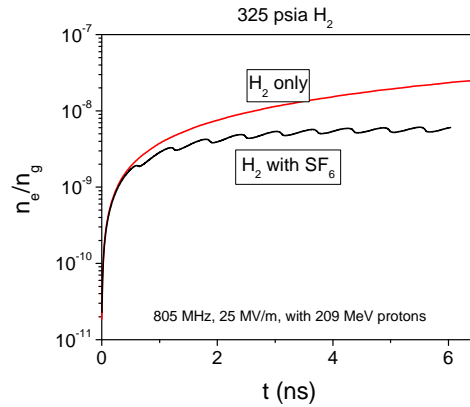


Figure 7: simulated electron density as a function of time in pure H_2 or (0.01%) SF_6 -doped H_2 with 209 MeV protons passing through at a rate similar to what will be expected in beam tests in the MTA.

The simulated electron density in the TC with an intense proton beam passing through it is shown in Figure 7. In the $\text{H}_2 + \text{SF}_6$ (0.01 %) condition, the electron density quickly reaches saturation and the density growth is stopped while the electron density in pure H_2 monotonically increases as a function of time. Note that twice the RF frequency can be seen in the doped curve, where the density drops when the field goes through zero. Beam tests with similar beam parameters of beam diameter and average intensity are planned in the Fall of 2009 at the MTA

CONCLUSION

Measurements of H_2 breakdown in the TC in the 325 psia Paschen region showed that (0.01 %) SF_6 doping increased the maximum stable gradient from about 25 to 38 MV/m as predicted by a numerical simulation. The simulation further predicts that such a small amount of SF_6 is sufficient to stop the growth of electron density in a high pressure RF cavity with a high intensity proton beam. This prediction will be tested at the Fermilab MTA as part of a program to develop cavities that will allow very efficient muon beam cooling.

REFERENCES

- [1] P. Hanlet et al., EPAC06, TUPCH147
- [2] A. Tollestrup, <http://beamdocs.fnal.gov/AD-public/DocDB/ShowDocument?docid=3345>
- [3] M. BastaniNejad et al., EPAC08, MOPP080
- [4] M. BastaniNejad et al., PAC09, WE5PFP008
- [5] C. Thoma, et al., IEEE Trans. Plasma Sci. 34, 910 (2006)
- [6] D. V. Rose, et al., Proc. 16th International Pulsed Power Conf., Albuquerque, New Mexico, 2007
- [7] D. V. Rose, C. Thoma, D. R. Welch, R. E. Clark, http://www.muonsinc.com/lemc2008/presentation/s/ROSE_LEMC2008.ppt